

# On resistance switching and oscillations in tubulin microtubule droplets

Alessandro Chiolerio<sup>a</sup>, Thomas C. Draper<sup>b</sup>, Richard Mayne<sup>b,c</sup>, Andrew Adamatzky<sup>b</sup>

<sup>a</sup>*Istituto Italiano di Tecnologia, Center for Sustainable Future Technologies, Via Livorno 60, 10144 Torino, Italy*

<sup>b</sup>*Unconventional Computing Laboratory, University of the West of England, Coldharbour Lane, Bristol, BS16 1QY, UK*

<sup>c</sup>*Department of Applied Sciences, University of the West of England, Coldharbour Lane, Bristol, BS16 1QY, UK*

---

## Abstract

We study electrical properties of Taxol-stabilised microtubule (MT) ensembles in a droplet of water. We demonstrate that the MT droplets act as electrical switches. Also, a stimulation of a MT droplet with a positive fast impulse causes oscillation of the droplet's resistance. The findings will pave a way towards future designs of MT-based sensing and computing devices, including data storage and featuring liquid state.

*Keywords:* Tubulin, Microtubules, Resistance switching, Oscillations, smart fluid systems

---

## 1. Introduction

The protein tubulin is a key component of the eukaryotic cytoskeleton [36, 41, 31]. The networks of tubulin microtubules (MTs) [47] are involved in cells' motility [20, 58, 24], intra-cellular transport [59, 51] and cell-level learning [26, 48, 37, 15, 53, 45, 18, 46, 33, 17]. In 1980 Hameroff and Rasmussen proposed that MT are responsible for a sub-cellular information processing [48, 28]. The framework of the sub-cellular computation was further supported by Priel, Tuszynski and Cantiello in their studies of information processing in actin-tubulin networks of neuron dendrites [45]. The pathways towards development of cytoskeleton based computing devices [4, 40, 38] have been so far mainly based on theoretical studies and computer modelling.

This might be explained by the fact that experimentally-wise it might be difficult to address individual units of tubulin polymers to write and read information arbitrarily. Therefore, at the present it might be reasonable to focus on ‘tubulin electronics’: designing of electronic components and circuits from MT networks with aim of their use in hybrid electro-mechanical analog computers. Another exciting framework is that of liquid robotics, where smart fluid systems could provide volume operation capabilities, being resilient to shape changes, impulse mechanical stresses, high pressures and radiation, and harsh environments in general [13]. The liquid state provides means for holographically addressing the information [42] and achieving much higher volume densities, also reducing routing dissipation and physical distance between bits of information [11]. There is also the scope to further ‘armour’ the droplets, by coating them with a hydrophobic powder, and thus form a ‘liquid marble’ [6, 19, 21]. Tuszynski and colleagues experimentally demonstrated memristive [56] and capacitive [34] electrical properties of a single MT. Priel and colleagues have experimentally shown, using patch-clamp technique, that MT exhibits electrical amplification and thus can act as bio-transistors [43]. Based on circumstantial evidences we can also claim that MT can act a variable resistors, because the conductivity of MT bundles can be controlled by stabilising and destabilising drugs [22].

Advancing our ideas on computing with vesicles filled with reactive cargo [2, 3, 30, 39] we decided to check electrical properties of MT networks in a bulk volume, i.e. a droplet. The paper presents an experimental setup, Sect. 2, for interfacing with MT droplets, and findings on electrical switching and resistance oscillations measured after submitting the droplet to a fast pulse waveform, Sect. 3. Applications of the findings are discussed in Sect. 4.

## 2. Experimental

Stabilised porcine brain microtubules (MTs) were supplied as a lyophilised powder. The MTs were reconstituted following the manufacture’s instructions [1], to yield the MTs. A buffer solution (10 mL) was made using deionised water (DIW, 15 M $\Omega$  cm), constituting 1,4-piperazinediethanesulfonic acid (PIPES, 15 mM), MgCl<sub>2</sub> (1 mM), and adjusted to pH 7.0 using NaOH. Separately, paclitaxel (Taxol) was dissolved in anhydrous dimethyl sulfoxide (DMSO) (100  $\mu$ L, 2 mM). The Taxol solution was then added to the buffer solution, forming the ‘resuspension buffer’ (RB). The RB (500  $\mu$ L) was then added to the lyophilised MT (500  $\mu$ g), followed by gentle stirring for

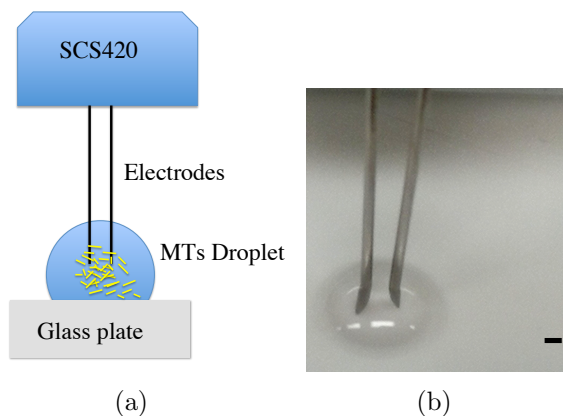


Figure 1: Scheme of the experiments (a) and a photo of MT droplet with electrodes inserted, bottom right: scale bar 2 mm (b).

10 minutes, yielding a final concentration of  $1 \text{ mg mL}^{-1}$ . Lyophilised MTs and Taxol were stored at  $3^\circ\text{C}$ , and all reaction steps were conducted at room temperature. Lyophilised MTs (#MT002, 99 %) and Taxol (#TXD01) were sourced from Cytoskeleton Inc; PIPES &  $\text{MgCl}_2$  were from Sigma-Aldrich; and NaOH was from Fisher Scientific. All reagents were used as received.

Electrical stimulation and recording was performed via needle electrodes composed of stainless steel coated by iridium, with twisted cable pairs (Spes Medica Srl, Italy). These electrodes were inserted 1 mm deep into the MT solution droplet, and the distance between them kept at 2 mm (Fig. 1). Fresh electrodes were used between each droplet, to prevent the effects of droplet evaporation and MT coating of the electrodes. The electronic characterisation was assessed using a Keithley Semiconductor Characterisation System SCS4200 with triaxial cables and preamplifiers. DC characterisation was conducted in the range  $[-1.2, +1.2]$  V. This limit was chosen to avoid the electrolysis of water at 1.23 V and oxidation of Taxol [25]. Alternated current (AC) measurements have been taken in the range from 1 kHz to 10 MHz, typically with a signal amplitude of 10 mV root-mean-square (RMS). By adding a direct current (DC) bias and sweeping it between two saturation values ( $-0.5$  V and  $+0.5$  V), impedance is measured at a fixed frequency with a small signal over-imposed (10 mV RMS).

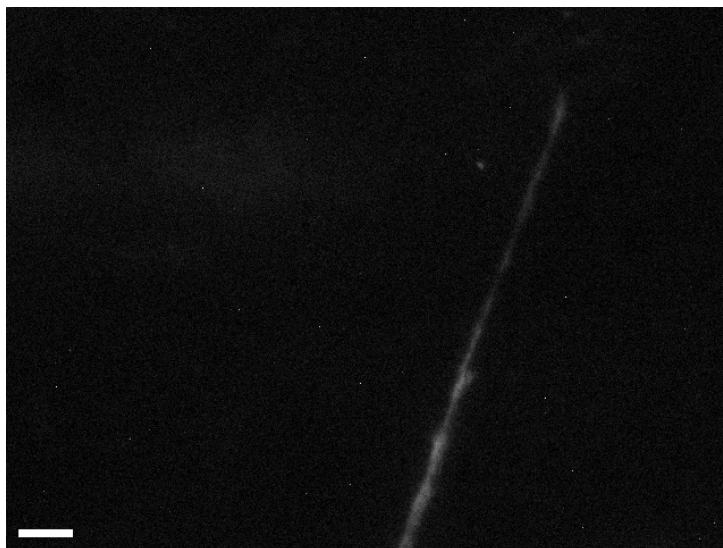
Pulse Train (PT) measurements featured a high speed pulse generator with internal reference and feedback system that is capable of measuring

its own output, plus two independent high speed voltage and current units connected to the device. By simultaneously monitoring the voltage and current at each of the electrodes, the effective resistive response is measured under the application of multiple unipolar pulses. The pulse is rectangular, has an amplitude of 0.5 V and a duration of 1 ms, selected to be comparable to biologic action potentials. The electrical response is recorded for a further 200  $\mu$ s, enabling us to trace the decay of the sample until rest condition (0 V). During each measurement the sample was submitted to a train of 50 pulses separated by 4 ms idle time and the resistive response was recorded and internally averaged; this procedure was repeated 10 times to trace any eventual drift and again averaged to compute the associated standard deviation.

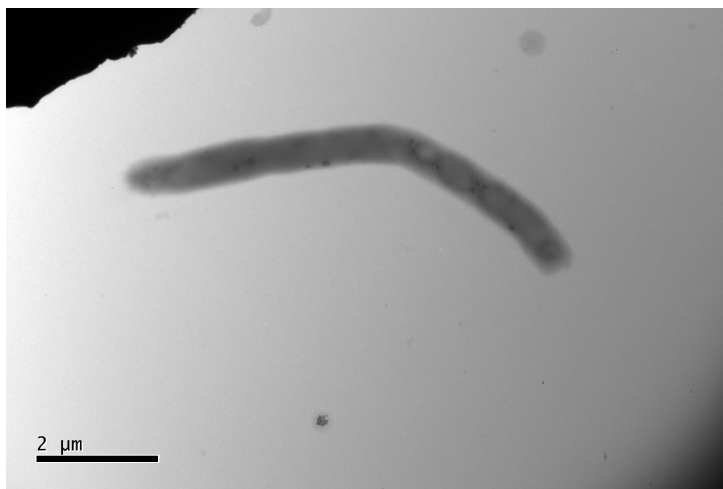
Microscopy was conducted on stabilised MT samples as follows. Samples of prepared MT were fixed in 1% glutaraldehyde in RB. Fluorescence microscopy was performed on a Zeiss Axiovert 200M inverted light microscope using a  $\times 100$  oil immersion lens, following staining with 1% 4,6-diamidino-2-phenylindole (DAPI) in DMSO; although best known as a nucleic acid stain, DAPI was here used for its affinity for tubulin associated in MTs [7]. 25  $\mu$ L samples were sandwiched between two 1.1 mm glass coverslips and excited with a CoolLed PE100 LED source. Images were collected using a Thorlabs 340M scientific CCD camera (Thorlabs, USA) and associated software. Samples were also observed using transmission electron microscopy (TEM) by adding 2.5  $\mu$ L of MT solution to a 400 square formvar-coated copper grid for 10 minutes, before adding 25  $\mu$ L of 1% uranyl acetate solution, for 30 seconds, after which the solution was blotted. The grids were left to dry, before being imaged in a Philips CM-10 TEM with a Gatan camera system.

### 3. Results

MTs were observed to exist as rod-shaped objects, as expected, via fluorescence microscopy, but were typically longer than their manufacturer-stated length when stabilised with Taxol, at over 10  $\mu$ m (Fig. 2)a. No structures correlating with the expected appearance of MT were observed via TEM, but rod-shaped objects that appeared to contain bundles of helically-arranged strings, measuring sub 100 nm and containing multiple electron-dense objects, were observed (Fig. 2b).



(a)



(b)

Figure 2: Microscopic appearance of MT samples. (a) Fluorescence micrograph to show a single stabilised MT. Scale bar 1.0  $\mu\text{m}$ . (b) TEM showing a rod-shaped helical arrangement, containing electron-dense objects (dark circles).

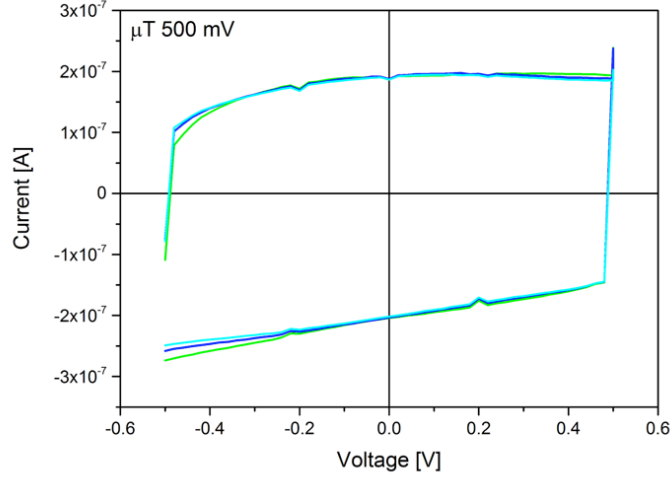


Figure 3: MT IV curve cycles

**Finding 1.** *MT droplet acts as an electrical switch.*

This was demonstrated by assessing DC properties of stabilised MT (stabilised as described in Sect. 2). Figure 3 shows three IV cycles measured in a range of 0.5 V. The cycle shows a substantial hysteresis and a maximum current of about 200 nA flowing through the sample, well above the DIW contribution which is one order of magnitude lower. Difference between the upcycle and the downcycle is particularly evident close to saturation: when the voltage is positive, in one case (quadrant IV) we have an associated differential resistance of 8.60 M $\Omega$  while in the other case (quadrant I) we have an associated (negative) differential resistance of -100 M $\Omega$ . Such negative differential resistance is usually associated to charge transfer phenomena between molecules close enough to enable electrostatic interaction to play a role [12].

**Finding 2.** *Stimulation of MT droplet with a positive impulse increases resistance of the droplets and causes oscillations of the droplet's resistance at the elevated level.*

DIW response to a unipolar pulse (Fig. 4(a)) is shown in Fig. 4(b), evidencing a noisy and rather flat resistance, with no distortion induced by high order harmonics.

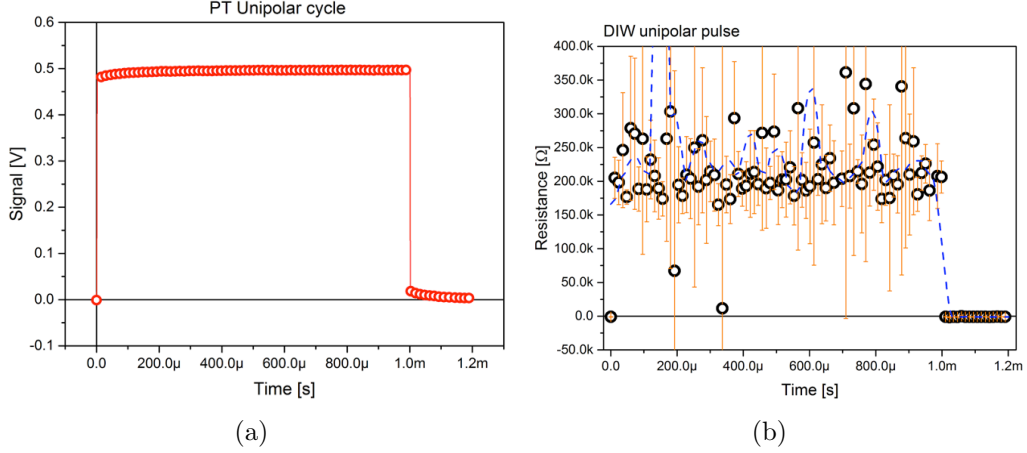
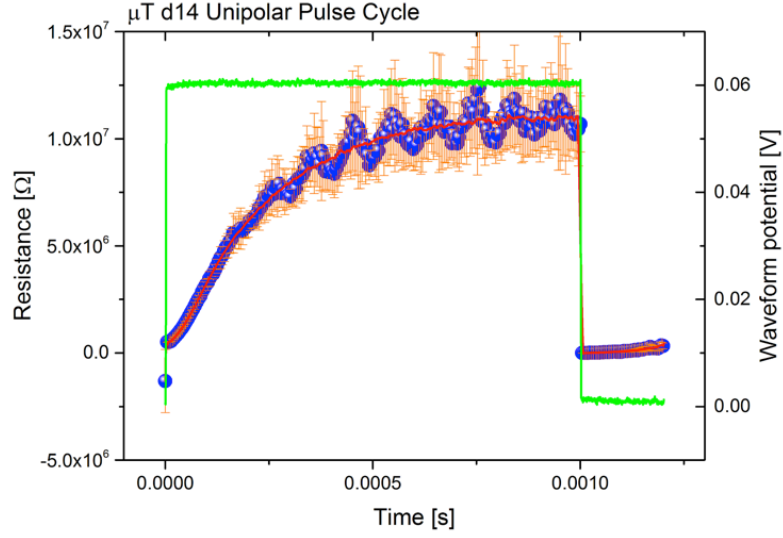


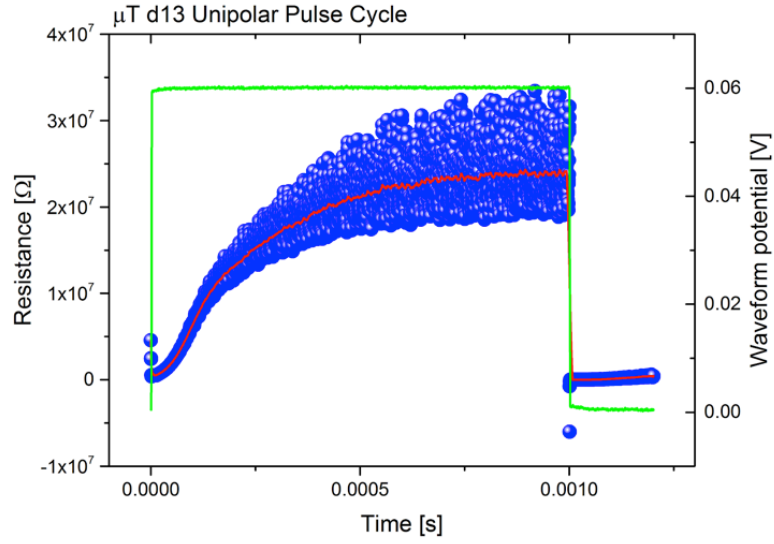
Figure 4: PT stimulation of a DIW droplet. (a) Unipolar pulse submitted to samples in the PT characterisation. (b) DIW response to the same (dashed line: adjacent averaging over 50 points). Ones point every 20 shown for clarity.

The rest resistance value is about  $950\ \Omega$ , that we may take as reference for further considerations on other materials. Figures 5(a) and 5(b) shows a comparison between the unipolar pulse response depending on pulse polarity. The positive pulse results (Fig. 5(a)) in a quite sharp response, plus an oscillating noise on the top profile. The negative pulse results in a very noisy response, rather chaotic (Fig. 5(b)).

Oscillations of the resistance are not pronounced on the the plot of responses to 100 positive impulses (Fig. 6(a)). The integrated responses to a bipolar stimulation does not show any coherent increase in resistance but a wide range of resistance values from  $0\ \Omega$  to nearly  $2 \times 10^8\ \Omega$ .



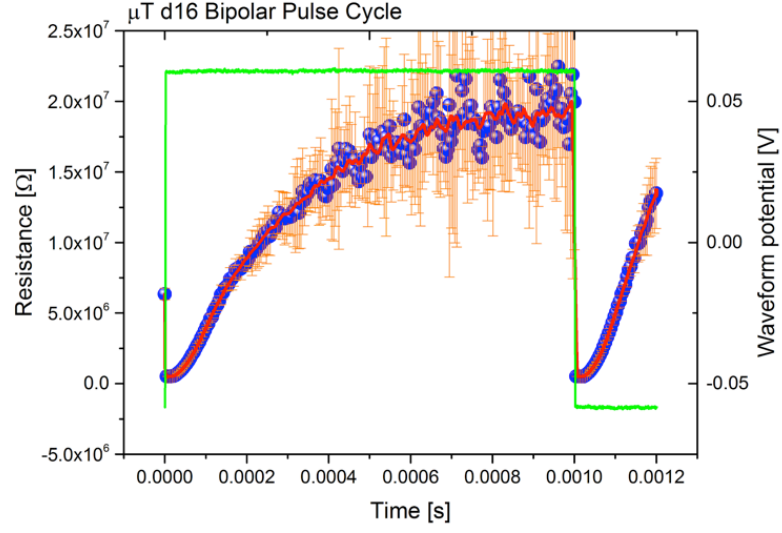
(a)



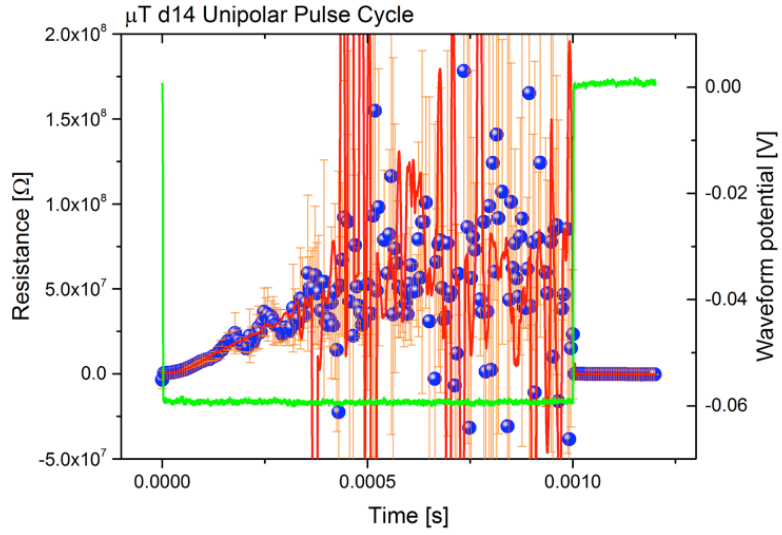
(b)

Figure 5: PT unipolar pulse positive (a), and negative (b), of a MT droplet. Only one point every 15 shown for clarity (blue). Average over six experimental curves superimposed to a smoothing over 51 adjacent points (red). Waveform potential shown in green. (a) Dynamics of the droplet resistance in a response to a positive impulse. (b) Dynamics of the droplet resistance in a response to a negative impulse.





(a)



(b)

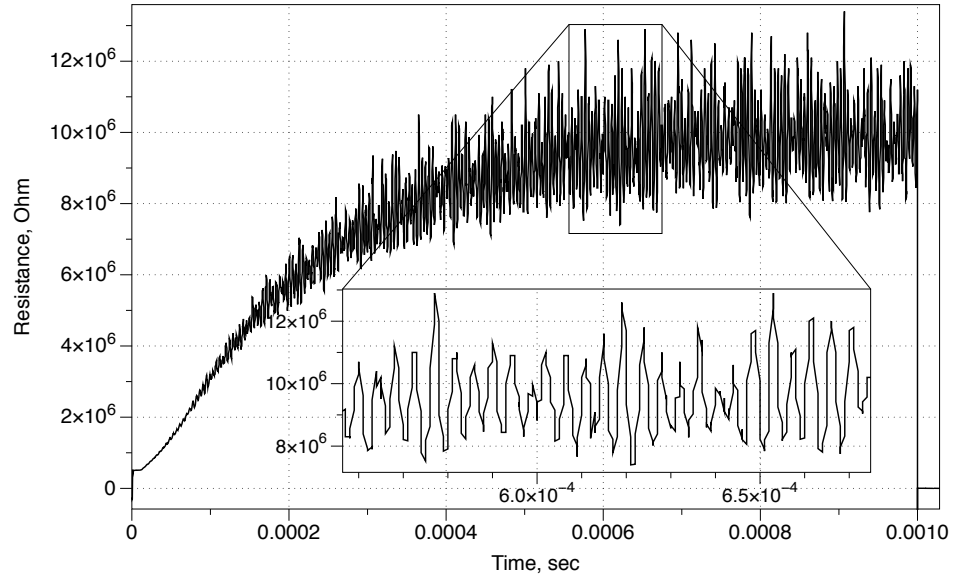
Figure 6: Dynamics of the MT droplet resistance in a response to (a) PT unipolar positive pulse after internal integration over 100 cycles, (b) PT bipolar. Only one point every 15 shown for clarity (blue). Waveform potential shown in green.

## 4. Discussions

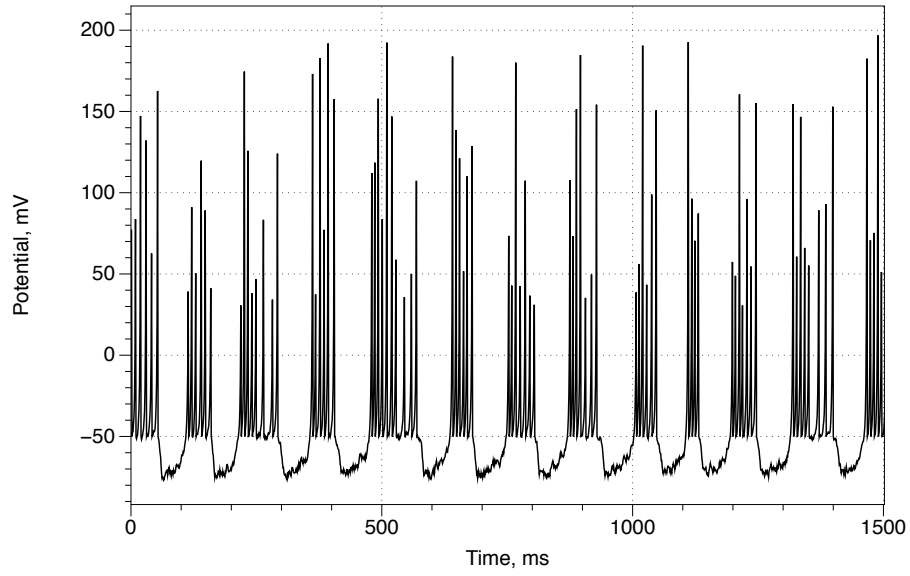
We demonstrated that MT droplets can show resistive switching in a limited range of voltages and trigger electronic oscillation under proper electrical stimulus, thus adding new members to a growing family of tubulin electronics [56, 56, 34, 22]. Future works could be focused on cascading tubulin electronic elements into purposeful electrical analog computing circuits.

Let us discuss potential mechanisms of the phenomena observed. What happens in the droplet? The Taxol molecule binds to each heterodimer in the MT. This binding makes the MT more rigid and helps prevent dissociation of the MT into individual heterodimers [60]. There are indications that Taxol-stabilised MTs self-organise into bundles of co-aligned tubes [52, 5]. Our TEM results on dehydrated Taxol-stabilised MT samples (Fig. 2b) would appear to at least partially support this hypothesis. The observed increase in the resistance of MT droplets could be due to the MTs self-organising into arrays of parallel tubes oriented along the lines of electro-magnetic field [57, 9, 23]. Let us evaluate a volume of MT networks used in our experiments. The radius of a MT is  $12.5 \text{ nm} = 1.25 \times 10^{-6} \text{ cm}$ . The length of the MT in the reconstructed solution, as per [1], can be taken as  $2 \text{ }\mu\text{m} = 2 \times 10^{-4} \text{ cm}$ . Thus the volume of one MT is  $9.82 \times 10^{-16} \text{ cm}^3$ . The total volume of all MT in each droplet, based on their concentration, is  $(1.66 \times 10^{10}) \times (9.82 \times 10^{-16}) = 1.63 \times 10^{-5} \text{ cm}^3$ . That is just  $1/613^{\text{th}}$  of the droplet volume is occupied by MT, yet, this amount is sufficient to exhibit non-trivial electrical properties in reason of their percolation threshold and their extremely elongated shape [10]. Note that whilst some MTs longer than  $2 \text{ }\mu\text{m}$  were detected, the concentration and quantity of tubulin in the droplet is fixed and finite, therefore the total occupied space remains unchanged.

The MT droplets exhibit oscillations of the resistance under applied positive voltage (Figs. 5(a) and 5(b) and Fig. 7(a)). An average period of a resistance spike is  $24 \text{ ns} (2.4 \times 10^{-5})$ , standard deviation  $0.4 \text{ ns}$ . The oscillations can be caused by electro-mechanical vibrations of the MT [29, 35], shuttling of conformation changes [27], orientation transitions of dipole moments [54, 8, 14], and ionic waves [55, 44, 50]. The oscillations show a visual resemblance to spiking of a chattering neuron in Izhikevich model [32] (Fig. 7(b)), yet the oscillations time scale is different by several orders of magnitude. Those faster oscillations could be the result of the much higher stiffness of MT bundles in Taxol-stabilised solutions. Further work is required to evaluate the possibility of integration of nano-seconds scale spiking in MT network into milli-seconds



(a)



(b)

Figure 7: (a) Oscillation of resistance. (b) Oscillation of a membrane potential of a computer model of chattering Izikevich neuron.

range spiking of neurons to understand better how exactly the MT oscillation can contribute to neuronal activity and information processing [16, 49].

## 5. Conclusions

We have demonstrated some of the electrical properties of aqueous Taxol-stabilised MTs. By applying a cycling DC potential and monitoring the current, we have indicated the electrical switch capabilities of the system, inherent in its large hysteresis. We have also revealed oscillations of the systems resistances, when exposed to the PT experiments. These oscillations could have a number of sources, and require further investigation. The findings add to the body of knowledge for MT-based systems, permitting further work in fields such as sensing, computing, and data storage.

## Acknowledgements

AC acknowledges Fondazione Istituto Italiano di Tecnologia for funding. Measurements were taken at the University of the West of England, Bristol, UK, while AC was visiting. AA and TCD were partly supported by the EPSRC with grant EP/P016677/1.

RM acknowledges Dr David Patton and Mrs Sue Hula of UWE Bristol for their invaluable expertise with the electron microscopical aspects of this work.

## References

## References

- [1] Data sheet. microtubules (taxol stabilized and lyophilized) cat. # MT002. <https://www.cytoskeleton.com/pdf-storage/datasheets/mt002.pdf>. Accessed: 7th April 2019.
- [2] Andrew Adamatzky, Ben De Lacy Costello, Julian Holley, Jerzy Gorecki, and Larry Bull. Vesicle computers: Approximating a voronoi diagram using voronoi automata. *Chaos, Solitons & Fractals*, 44(7):480–489, 2011.
- [3] Andrew Adamatzky, Julian Holley, Larry Bull, and Ben De Lacy Costello. On computing in fine-grained compartmentalised belousov–zhabotinsky medium. *Chaos, Solitons & Fractals*, 44(10):779–790, 2011.

- [4] Andrew Adamatzky, Jack Tuszynski, Joerg Pieper, Dan V Nicolau, Rossalia Rinaldi, Georgios Sirakoulis, Victor Erokhin, Joerg Schnauss, and David M Smith. Towards cytoskeleton computers. a proposal. *arXiv preprint arXiv:1810.04981*, 2018.
- [5] JM Andreu, Joan Bordas, JF Diaz, J Garcia de Ancos, R Gil, Francisco J Medrano, Eva Nogales, E Pantos, and Elizabeth Towns-Andrews. Low resolution structure of microtubules in solution: Synchrotron x-ray scattering and electron microscopy of taxol-induced microtubules assembled from purified tubulin in comparison with glycerol and map-induced microtubules. *Journal of molecular biology*, 226(1):169–184, 1992.
- [6] Pascale Aussillous and David Quéré. Liquid marbles. *Nature*, 411(6840):924–927, 2001.
- [7] Heuséle C Bonne, D, C Simon, and D Pantaloni. 4',6-diamidino-2-phenylindole, a fluorescent probe for tubulin and microtubules. *Journal of Biological Chemistry*, 260(5), 1985.
- [8] JA Brown and JA Tuszynski. Dipole interactions in axonal microtubules as a mechanism of signal propagation. *Physical Review E*, 56(5):5834, 1997.
- [9] JA Brown and JA Tuszynski. A review of the ferroelectric model of microtubules. *Ferroelectrics*, 220(1):141–155, 1999.
- [10] Micaela Castellino, Alessandro Chiolerio, Shahzad Muhammad Imran, Pravin Vitthal Jagdale, and Alberto Tagliaferro. Electrical conductivity phenomena in an epoxy resin–carbon-based materials composite. *Composites: Part A*, 61:108–114, 2014.
- [11] Alessandro Chiolerio, Thomas C. Draper, Carsten Jost, and Andrew Adamatzky. Electrical properties of solvated tectomers: Towards zettascale computing. *Advanced Electronic Materials*, submitted to, 2019.
- [12] Alessandro Chiolerio, Samuele Porro, and Sergio Bocchini. Impedance hyperbolicity in inkjet-printed graphene nanocomposites: Tunable capacitors for advanced devices. *Advanced Electronic Materials*, 2:1500312, 2016.

- [13] Alessandro Chiolerio and Marco B. Quadrelli. Smart fluid systems: The advent of autonomous liquid robotics. *Advanced Science*, 4:1700036, 2017.
- [14] Michal Cifra, Jirí Pokorný, Daniel Havelka, and O Kučera. Electric field generated by axial longitudinal vibration modes of microtubule. *BioSystems*, 100(2):122–131, 2010.
- [15] Michael Conrad. Cross-scale information processing in evolution, development and intelligence. *BioSystems*, 38(2):97–109, 1996.
- [16] Travis John Adrian Craddock and Jack A Tuszynski. A critical assessment of the information processing capabilities of neuronal microtubules using coherent excitations. *Journal of biological physics*, 36(1):53, 2010.
- [17] Judith Dayhoff, Stuart Hameroff, Rafael Lahoz-Beltra, and Charles E Swenberg. Cytoskeletal involvement in neuronal learning: A review. *European biophysics journal*, 23(2):79–93, 1994.
- [18] Dominique Debanne. Information processing in the axon. *Nature Reviews Neuroscience*, 5(4):304–316, 2004.
- [19] Thomas C. Draper, Claire Fullarton, Richard Mayne, Neil Phillips, Giacomo E. Canciani, Ben P. J. de Lacy Costello, and Andrew Adamatzky. Mapping outcomes of liquid marble collisions. *Soft Matter*, 15(17):3541–3551, 2019.
- [20] Daniel A Fletcher and R Dyche Mullins. Cell mechanics and the cytoskeleton. *Nature*, 463(7280):485, 2010.
- [21] Claire Fullarton, Thomas C. Draper, Neil Phillips, Richard Mayne, Ben P. J. de Lacy Costello, and Andrew Adamatzky. Evaporation, Lifetime, and Robustness Studies of Liquid Marbles for Collision-Based Computing. *Langmuir*, 34(7):2573–2580, 2018.
- [22] Milad Gharooni, Alireza Alikhani, Hassan Moghtaderi, Hamed Abiri, Alireza Mashaghi, Fereshteh Abbasvandi, Mohammad Ali Khayamian, Zohreh sadat Miripour, Ashkan Zandi, and Mohammad Abdollahad. Bioelectronics of the cellular cytoskeleton: Monitoring cytoskeletal conductance variation for sensing drug resistance. *ACS sensors*, 2019.

- [23] Nicolas Glade and James Tabony. Brief exposure to high magnetic fields determines microtubule self-organisation by reaction–diffusion processes. *Biophysical chemistry*, 115(1):29–35, 2005.
- [24] Tom Golde, Constantin Huster, Martin Glaser, Tina Händler, Harald Herrmann, Josef A. Käs, and Jörg Schnauß. Glassy dynamics in composite biopolymer networks. *Soft Matter*, -(-):-, 2018.
- [25] Jayant I. Gowda and Sharanappa T. Nandibewoor. Electrochemical behavior of paclitaxel and its determination at glassy carbon electrode. *Asian J. Pharm. Sci.*, 9(1):42–49, feb 2014.
- [26] SR Hameroff. Coherence in the cytoskeleton: Implications for biological information processing. In *Biological coherence and response to external stimuli*, pages 242–265. Springer, 1988.
- [27] Stuart Hameroff, Alex Nip, Mitchell Porter, and Jack Tuszynski. Conduction pathways in microtubules, biological quantum computation, and consciousness. *Biosystems*, 64(1-3):149–168, 2002.
- [28] Stuart Hameroff and Steen Rasmussen. Microtubule automata: Sub-neural information processing in biological neural networks, 1990.
- [29] Daniel Havelka, Michal Cifra, and Ondřej Kučera. Multi-mode electro-mechanical vibrations of a microtubule: In silico demonstration of electric pulse moving along a microtubule. *Applied Physics Letters*, 104(24):243702, 2014.
- [30] Julian Holley, Andrew Adamatzky, Larry Bull, Ben De Lacy Costello, and Ishrat Jahan. Computational modalities of belousov–zhaborotinsky encapsulated vesicles. *Nano Communication Networks*, 2(1):50–61, 2011.
- [31] Florian Huber, Jörg Schnauß, Susanne Rönicke, Philipp Rauch, Karla Müller, Claus Fütterer, and Josef A. Käs. Emergent complexity of the cytoskeleton: from single filaments to tissue. *Advances in Physics*, 62(1):1–112, 2013.
- [32] Eugene M Izhikevich. Simple model of spiking neurons. *IEEE Transactions on neural networks*, 14(6):1569–1572, 2003.

- [33] Laurent Jaeken. A new list of functions of the cytoskeleton. *IUBMB life*, 59(3):127–133, 2007.
- [34] Aarat Kalra, Sahil Patel, Asadullah Bhuiyan, Jordane Preto, Kyle Scheuer, Usman Mohammed, John Lewis, Vahid Rezaia, Karthik Shankar, and Jack A Tuszynski. On the capacitive properties of individual microtubules and their meshworks. *arXiv preprint arXiv:1905.02865*, 2019.
- [35] Si Li, Chengyuan Wang, and Perumal Nithiarasu. Electromechanical vibration of microtubules and its application in biosensors. *Journal of the Royal Society Interface*, 16(151):20180826, 2019.
- [36] Jan Löwe, H Li, KH Downing, and E Nogales. Refined structure of  $\alpha\beta$ -tubulin at 3.5 Å resolution. *Journal of molecular biology*, 313(5):1045–1057, 2001.
- [37] Beat Ludin and Andrew Matus. The neuronal cytoskeleton and its role in axonal and dendritic plasticity. *Hippocampus*, 3(S1):61–71, 1993.
- [38] Richard Mayne and Andrew Adamatzky. Cellular automata modelling of slime mould actin network signalling. *Natural Computing*, 18(1):5–12, 2019.
- [39] Richard Mayne and Andrew Adamatzky. On the computing potential of intracellular vesicles. *PloS one*, 10(10):e0139617, 2015.
- [40] Richard Mayne, Andrew Adamatzky, and Jeff Jones. On the role of the plasmodial cytoskeleton in facilitating intelligent behaviour in slime mould *Physarum polycephalum*. *Communicative and Integrative Biology*, 8(4):e1059007, 2015.
- [41] Thomas D Pollard and Robert D Goldman, editors. *The Cytoskeleton*, volume 1. Springer, 2010.
- [42] K. Jr. Preston. Digital holographic logic. *Pattern Recognition*, 5:37–49, 1973.
- [43] Avner Priel, Arnolt J Ramos, Jack A Tuszynski, and Horacio F Cantiello. A biopolymer transistor: electrical amplification by microtubules. *Biophysical journal*, 90(12):4639–4643, 2006.



- [44] Avner Priel, Jack A Tuszynski, and Horacio F Cantiello. Ionic waves propagation along the dendritic cytoskeleton as a signaling mechanism. *Advances in Molecular and Cell Biology*, 37:163–180, 2006.
- [45] Avner Priel, Jack A Tuszynski, and Horacion F Cantiello. The dendritic cytoskeleton as a computational device: an hypothesis. In *The emerging physics of consciousness*, pages 293–325. Springer, 2006.
- [46] Avner Priel, Jack A Tuszynski, and Nancy J Woolf. Neural cytoskeleton capabilities for learning and memory. *Journal of biological physics*, 36(1):3–21, 2010.
- [47] Daniel L Purich and David Kristofferson. Microtubule assembly: a review of progress, principles, and perspectives. *Adv. Protein Chem*, 36:133–212, 1984.
- [48] Steen Rasmussen, Hasnain Karampurwala, Rajesh Vaidyanath, Klaus S Jensen, and Stuart Hameroff. Computational connectionism within neurons: A model of cytoskeletal automata subserving neural networks. *Physica D: Nonlinear Phenomena*, 42(1-3):428–449, 1990.
- [49] V Salari, J Tuszynski, I Bokkon, M Rahnama, and M Cifra. On the photonic cellular interaction and the electric activity of neurons in the human brain. In *Journal of Physics: Conference Series*, volume 329, page 012006. IOP Publishing, 2011.
- [50] MV Satarić, DI Ilić, N Ralević, and Jack Adam Tuszynski. A nonlinear model of ionic wave propagation along microtubules. *European biophysics journal*, 38(5):637–647, 2009.
- [51] Melina Schuh. An actin-dependent mechanism for long-range vesicle transport. *Nature cell biology*, 13(12):1431, 2011.
- [52] M Somers and Yves Engelborghs. Kinetics of the spontaneous organization of microtubules in solution. *European Biophysics Journal*, 18(4):239–244, 1990.
- [53] JA Tuszynski, JA Brown, and P Hawrylak. Dielectric polarization, electrical conduction, information processing and quantum computation in microtubules. are they plausible? *Philosophical Transactions – Royal*

*Soc Series A. Mathematical, Physical and Engineering Sciences*, pages 1897–1925, 1998.

- [54] JA Tuszyński, S Hameroff, MV Satarić, B Trpisova, and MLA Nip. Ferroelectric behavior in microtubule dipole lattices: implications for information processing, signaling and assembly/disassembly. *Journal of Theoretical Biology*, 174(4):371–380, 1995.
- [55] JA Tuszyński, S Portet, JM Dixon, C Luxford, and HF Cantiello. Ionic wave propagation along actin filaments. *Biophysical journal*, 86(4):1890–1903, 2004.
- [56] Jack Tuszyński. Microtubule iv characteristics are consistent with memristor-like behavior. 2016.
- [57] Peter M Vassilev, Reni T Dronzine, Maria P Vassileva, and Georgi A Georgiev. Parallel arrays of microtubules formed in electric and magnetic fields. *Bioscience reports*, 2(12):1025–1029, 1982.
- [58] Miguel Vicente-Manzanares and Alan Rick Horwitz. Cell migration: an overview. In *Cell migration*, pages 1–24. Springer, 2011.
- [59] Dieter Volkmann and František Baluška. Actin cytoskeleton in plants: from transport networks to signaling networks. *Microscopy research and technique*, 47(2):135–154, 1999.
- [60] Hui Xiao, Pascal Verdier-Pinard, Narcis Fernandez-Fuentes, Berta Burd, Ruth Angeletti, Andras Fiser, Susan Band Horwitz, and George A Orr. Insights into the mechanism of microtubule stabilization by Taxol. *Proceedings of the National Academy of Sciences*, 103(27):10166–10173, 2006.